

High magnetization FeCo/Pd multilayers

M. J. Walock^{a)}

Center for Materials for Information Technology and Department of Physics and Astronomy, The University of Alabama, Tuscaloosa, Alabama 35487-0209

H. Ambaye

Spallation Neutron Source, Oak Ridge National Laboratory, Oak Ridge, Tennessee 37831-6745

M. Chshiev

Center for Materials for Information Technology and Department of Physics and Astronomy, The University of Alabama, Tuscaloosa, Alabama 35487-0209

F. R. Klose

Spallation Neutron Source, Oak Ridge National Laboratory, Oak Ridge, Tennessee 37831-6745

W. H. Butler and G. J. Mankey

Center for Materials for Information Technology and Department of Physics and Astronomy, The University of Alabama, Tuscaloosa, Alabama 35487-0209

(Received 1 October 2007; accepted 19 November 2007; published 30 June 2008)

We have fabricated multilayer samples with varying superlattice periodicity and interlayer thicknesses to determine the nature of the enhanced moment in this intriguing thin film system. Magnetic characterization experiments show an enhanced magnetic moment in the multilayers as compared to a single layer film containing the same amount of FeCo. However, since the magnetization is defined as the magnetic moment divided by the sample volume, the sample exhibits an overall reduction in the magnetization when the volume of the Pd layers is also taken into account. Our experimental findings are also supported by theoretical calculations which identify the origin of the increased magnetic moment in the multilayer system. Polarized neutron reflectivity experiments will be used to determine the lateral distribution of the magnetization in a number of superlattice samples. © 2008 American Vacuum Society. [DOI: 10.1116/1.2830631]

I. INTRODUCTION

A high saturation magnetization is very advantageous in magnetic recording. Among the 3d ferromagnetic materials, the FeCo bcc-alloy system has the highest known magnetic moment along the Slater-Pauling curve.¹ As a result, this group of materials are widely used in the magnetic recording industry. However, recent advances in areal storage density have stretched this system to its magnetic limit. Further advances will require either a new class of materials or improvements on the current set. Here, we investigate a possible method of improvement on the current set of FeCo bcc alloys.

Increasing the saturation magnetization of FeCo alloys is a possible answer. This may be accomplished by adding Pd, either as an impurity or as a thin spacer layer within a superlattice. In the case of pure Fe, the addition of Pd, either as an impurity or as a thin film in a multilayer structure, reveals an increase in the Fe magnet moment. This is due to interfacial mixing of the Fe 3d and Pd 4d majority spin channels. This mixing results in an increased moment on the Fe and an induced moment on the Pd.² While the interaction between Fe and Pd has been well documented,³⁻⁷ there is little research on the introduction of Pd into FeCo.^{8,9} This article reports on the structural and magnetic properties of a Fe₆₅Co₃₅/Pd heterostructure.

II. EXPERIMENT

The samples consisted of $n=1$ and 16 repetitions of Fe₆₅Co₃₅/Pd on 1 cm², a -plane sapphire substrates, with a 6.7 nm Cr buffer layer and a 5 nm Pd capping layer. The Fe₆₅Co₃₅ and Pd thicknesses were adjusted to maintain total thicknesses of 9.76 and 4.0 nm, respectively. All the samples were prepared in a dc magnetron sputtering system, with a

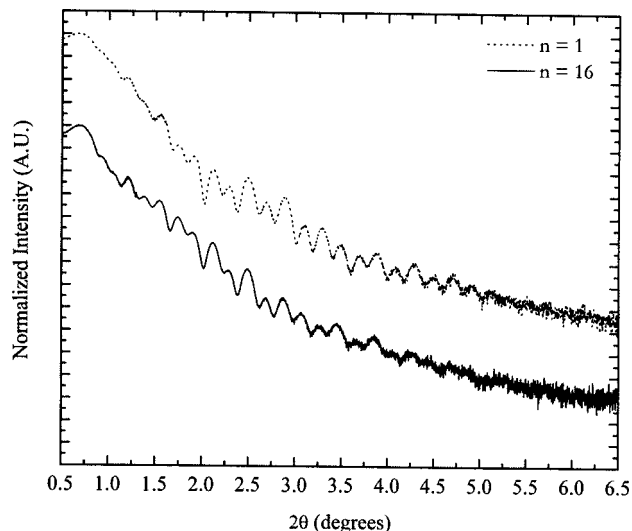


FIG. 1. X-ray reflectivity spectra of the single layer ($n=1$) and multilayer ($n=16$) Fe₆₅Co₃₅/Pd samples.

^{a)}Electronic mail: waloc001@bama.ua.edu

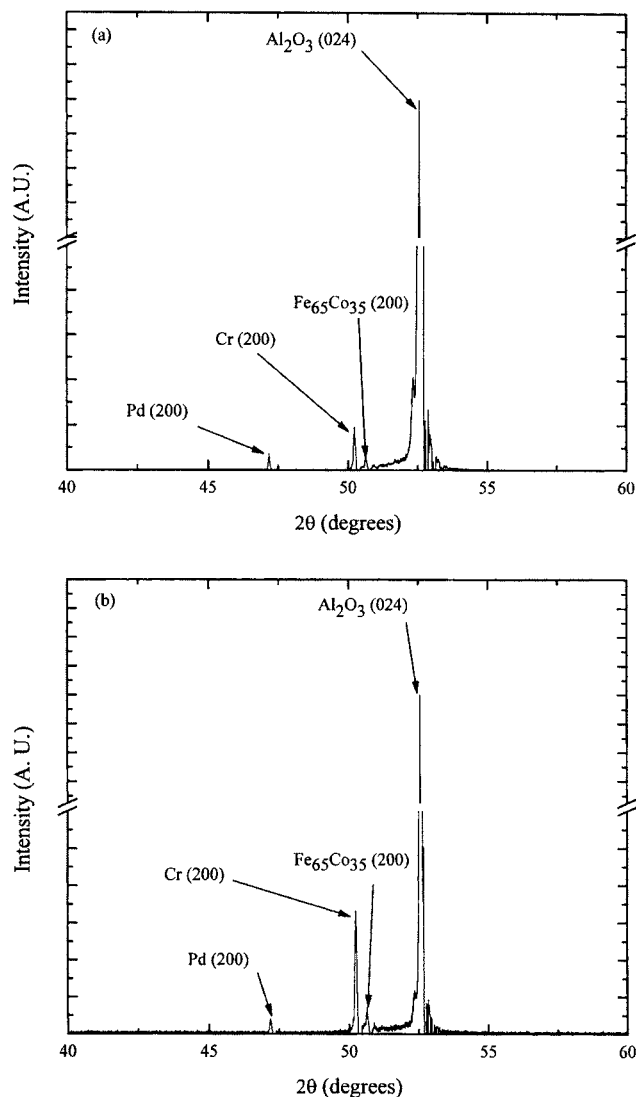


FIG. 2. X-ray diffraction patterns of the (a) single layer and (b) multilayer $\text{Fe}_{65}\text{Co}_{35}/\text{Pd}$ samples.

base pressure of $6.6(10^{-7})$ Pa and an argon-working pressure of 0.36 Pa. All targets have greater than 99.9% purity. A quartz crystal microbalance calibrated the deposition rates of Cr, $\text{Fe}_{65}\text{Co}_{35}$, and Pd at 0.067, 0.15, and 0.033 nm/s, respec-

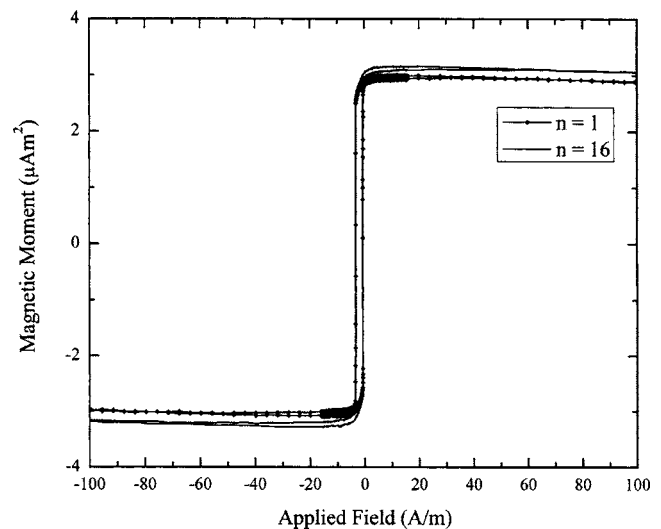


FIG. 3. Hysteresis loops of the single layer and multilayer $\text{Fe}_{65}\text{Co}_{35}/\text{Pd}$ samples. The saturation moments are for the $n=1$ and $n=16$ samples, respectively.

tively. The resulting multilayer samples were structurally characterized by x-ray reflectivity and diffraction. A DMS model 1660 vibrating sample magnetometer was used for the magnetic characterization.

III. RESULTS AND DISCUSSION

A. Structural characterization

Structural characterization was carried out on a Philips X'Pert MPD Pro diffractometer with a $\text{Cu } K\alpha$ radiation source. The geometry of x-ray reflectivity (XRR) and x-ray diffraction (XRD) are similar with one exception. For XRR, there is a glancing angle of incidence, $0^\circ < 2\theta < 10^\circ$. For XRD, the angle of incidence is higher, greater than $2\theta > 10^\circ$. Reflectivity curves, as shown in Fig. 1, are fitted to determine sample thickness, density, and interfacial roughness. Once acquired, the data is fit¹⁰ to a sample model using Parratt recursive formalism,¹¹ with a Névo-Croce error function accounting for the interfacial roughness.¹² Typical results are presented in Fig. 1. The fitting program yielded layer thicknesses which deviated from the nominal thick-

TABLE I. X-ray reflectivity results for the single layer ($n=1$) and multilayer ($n=16$) $\text{Fe}_{65}\text{Co}_{35}/\text{Pd}$ samples.

Sample	Material	Periodicity	Thickness (nm)	Roughness (nm)	Density (kg/m^3)	Atomic number
$n=1$	Cr	1	7.175	0.01	7896.72	23.8
	$\text{Fe}_{65}\text{Co}_{35}$	1	9.365	0.01	9329.15	24.6
	Pd	1	7.478	0.019	12194.92	45.9
	PdO_x	1	1.479	0.46	10900.28	3.0
$n=16$	Cr	1	10.351	2.77	6415.58	23.8
	$\text{Fe}_{65}\text{Co}_{35}$	16	9.941	0.14	8405.67	24.6
	Pd	15	5.156	0.22	9609.96	45.9
	Pd	1	2.053	0.01	13450.09	45.9
	PdO_x	1	1.013	0.03	7731.49	3.0

TABLE II. Magnetic characterization results for the single layer and multilayer Fe₆₅Co₃₅/Pd samples.

Sample	Magnetic moment (μAm^2)	Using only Fe ₆₅ Co ₃₅		Using Fe ₆₅ Co ₃₅ and Pd		Magnetization at absolute zero
		Magnetic volume (m^3)	Magnetization (kA/m)	Magnetic volume (m^3)	Magnetization (kA/m)	
$n=1$	3.0 ± 0.15	$(9.365 \pm 0.03) \times 10^{-13}$	320 ± 10	$(9.365 \pm 0.03) \times 10^{-13}$	320 ± 10	350 ± 11
$n=16$	3.17 ± 0.16	$(9.941 \pm 0.03) \times 10^{-13}$	320 ± 12	$(15 \pm 3) \times 10^{-13}$	200 ± 50	230 ± 50

nesses. These deviations, which are summarized in Table I, result in a 6% variation in the Fe₆₅Co₃₅ volume, and a 4% variation in the Pd volume, between the samples. The fitting also revealed an oxide layer of about 1.5 nm on the surface of the samples.

XRD scans in the 2θ - θ mode on the multilayer structures are used to identify the crystallographic phases, as shown in Fig. 2. The Pd layers are found in the fcc phase, with a lattice constant of 0.385 nm. The Fe₆₅Co₃₅ layers are in the bcc

phase with a lattice constant of 0.360 nm. Careful inspection of the peak positions indicates that the Fe₆₅Co₃₅ and Pd lattice constants remain constant with increasing interfaces.

B. Magnetic Characterization

The use of Pd in a multilayer has a significant effect on the magnetic environment. Figure 3 shows the room temperature VSM results for the multilayer sample and the reference sample, which are further summarized in Table II. There is a clear enhancement of the magnetic moment of the $n=16$ sample. However, if we calculate the magnetization, the moment per unit volume, using only the volume of the Fe₆₅Co₃₅ layers, the magnetization is only enhanced by 0.18% for the $n=16$ sample. However, once the Pd volume is included in the calculation of magnetization, the overall magnetization decreases by 53%. From a qualitative point of view, these results are in agreement with our theoretical calculations.¹³

While these results are enticing, the accuracy of our magnetization measurements and the resulting moment calculations pose problems. While the sample area was constant within 0.2%, the x-ray reflectivity curves determined that the Fe₆₅Co₃₅ thicknesses varied by 2% and 4%, for $n=1$ and $n=16$, respectively. As there is some uncertainty in the XRR fitting, we can place an uncertainty of approximately 5.5% in the determination of the magnetization. This uncertainty in the magnetization is on the same order as the observed magnetic moment enhancement.

All of the measurements presented here were taken at room temperature. If we assume that the magnetization follows a temperature dependent phenomenological power law with an exponent of 0.37 ± 0.02 ,¹⁴ and that phenomenological the Fe₆₅Co₃₅ layers have a Curie temperature of 1250 °C, then the zero temperature magnetization will increase by 9.4%. We would expect that the Fe₆₅Co₃₅ layers would have a bulklike Curie temperature since the predictions of the finite-size scaling model show a marked decrease in the Curie temperature only for films less than 0.34 nm thick.¹⁵ Thus, we can conservatively estimate that the zero temperature magnetization will be approximately 9% larger than the room temperature values.

C. Polarized neutron reflectometry

Our theoretical calculations¹³ and other experimental results^{2,3} show the origin of the enhanced magnetization is an induced magnetic moment on the Pd layers. We plan to use polarized neutron reflectivity (PNR) to detect the origin of

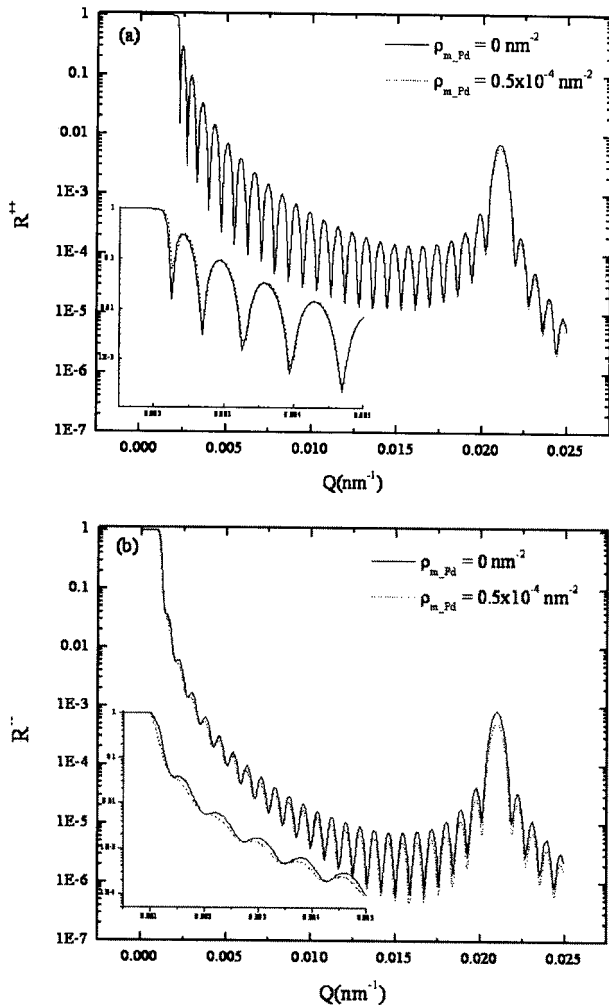


FIG. 4. Simulated polarized neutron reflectivity results depicting the non-spin-flip reflectivity states, (a) R^{++} and (b) R^{--} , of a 25-layer Fe₇₀Co₃₀ (2.0 nm)/Pd (1.0 nm) sample. The inset graphs illustrate the area in vicinity of the critical angle. The Fe₇₀Co₃₀ has a magnetic scattering length density of $4.71 \times 10^{-4} \text{ nm}^{-2}$; the Pd has a magnetic scattering length density of $0.5 \times 10^{-4} \text{ nm}^{-2}$.

the enhanced moment of this system. PNR can be used to determine the interfacial structure, magnetic roughness, and the distribution of the magnetization vector within multilayer samples.¹⁶ This is accomplished by comparing the spin-flip states and non-spin-flip states of the neutrons.¹⁷

We have performed simulations¹⁸ to show the sensitivity of the Vertical Surface Magnetism Reflectometer, Spallation Neutron Source Beamline 4A, is sufficient to resolve the differences in the neutron reflectivity. We used the stacking order developed by Noma *et al.*^{1,2} to simulate the multilayer sample. Figure 4 shows simulated PNR results for a 25-bilayer system of Fe₇₀Co₃₀ (2.0 nm)/Pd (1.0 nm); the magnetic scattering length density of the Fe₇₀Co₃₀ is $4.71 \times 10^{-4} \text{ nm}^{-2}$. In the case of an induced Pd moment, the magnetic scattering length density is $0.5 \times 10^{-4} \text{ nm}^{-2}$. The relatively small layer dimensions and low magnetic scattering length density of Pd were chosen to demonstrate an extremely low effect in the reflectivity spectra. The simulations demonstrate that the range of the reflectivity can be observed with the instrument in its current status.

IV. CONCLUSIONS AND FUTURE WORK

Multilayer samples of Fe₆₅Co₃₅/Pd were characterized in order to investigate the magnetic moment enhancement reported in the system. Our theoretical calculations show an increase in the magnetization of the Fe₆₅Co₃₅ layers and a decrease in the overall magnetization. Our experimental results confirm the decrease in the overall magnetization of the system. However, we cannot confirm the increase in the Fe₆₅Co₃₅ layer magnetization. Our future work will attempt to confirm the theoretical results through polarized neutron reflectivity.

ACKNOWLEDGMENTS

This research work was funded by the U.S. Department of Energy and by NSF Materials Research Science and Engineering Center program through Grant No. NSF-DMR 0213985. This work was also partly supported by Oak Ridge National Laboratory, managed by UT-Battelle, LLC, for the U.S. Department of Energy under Contract No. DE-AC05-00OR22725.

¹L. Pauling, Phys. Rev. **54**, 899 (1938).

²J. Vogel, A. Fontaine, V. Cros, F. Petroff, J.-P. Kappler, G. Krill, A. Rogalev, and J. Goulon, J. Magn. Magn. Mater. **165**, 96 (1997).

³L. Cheng, Z. Altounian, D. H. Ryan, J. O. Ström-Olsen, M. Sutton, and Z. Tun, Phys. Rev. B **69**, 144403 (2004).

⁴J. F. van Acker, P. J. W. Weijs, J. C. Fuggle, K. Horn, H. Haak, and K. H. J. Buschow, Phys. Rev. B **43**, 8903 (1991).

⁵O. Rader, C. Carbone, W. Clemens, E. Vescovo, S. Blügel, W. Eberhardt, and W. Gudat, Phys. Rev. B **45**, 13823 (1992).

⁶B. Hillebrands, A. Boufelfel, C. M. Falco, P. Baumgart, G. Güntherodt, E. Zimgiebl, and J. D. Thompson, J. Appl. Phys. **63**, 3880 (1988).

⁷E. Holmström, L. Nordström, and A. M. N. Niklasson, Phys. Rev. B **67**, 184403 (2003).

⁸K. Noma, M. Matsuoka, H. Kanai, Y. Uehara, K. Nomura, and N. Awaji, IEEE Trans. Magn. **42**, 140 (2006).

⁹K. Noma, M. Matsuoka, H. Kanai, Y. Uehara, K. Nomura, and N. Awaji, IEEE Trans. Magn. **41**, 2920 (2005).

¹⁰D. K. G. de Boer and A. J. G. Leenaers, WINGIXA simulation software, Philips Analytical, Eindhoven, The Netherlands, 1996.

¹¹L. G. Parratt, Phys. Rev. **95**, 359 (1954).

¹²L. Nevót and P. Croce, Rev. Phys. Appl. **15**, 761 (1980).

¹³M. Chshiev and W. H. Butler, Presented at the Center for Materials for Information Technology Fall Review, The University of Alabama, Tuscaloosa, AL 2006 (unpublished).

¹⁴V. V. Krishnamurthy, I. Zoto, G. J. Mankey, J. L. Robertson, S. Maat, E. E. Fullerton, I. Nwagwu, and J. K. Akujieze, Phys. Rev. B **70**, 024424 (2004).

¹⁵B. Nickel, W. Donner, H. Dosch, C. Detlefs, and G. Grübel, Phys. Rev. Lett. **85**, 134 (2000).

¹⁶H. Zabel, Mater. Today **9**, 42 (2006).

¹⁷J. F. Ankner and G. P. Felcher, J. Magn. Magn. Mater. **200**, 741 (1999).

¹⁸C. Braun, PARRATT32 simulation software, HMI, Berlin, Germany, 1997.